Non-uniqueness of the multi-temperature law of mass action. Application to 2T plasma composition calculation by means of a collisional-radiative model

Julien Annaloro, Philippe Teulet, Arnaud Bultel, Yann Cressault, Alain Gleizes

Non-uniqueness of the multi-temperature law of mass action. Application to 2T plasma composition calculation by means of a collisional-radiative model

Julien Annaloro[1,2,a], Philippe Teulet[1,b], Arnaud Bultel[2], Yann Cressault[1], and Alain Gleizes[1]

[1] Université de Toulouse, UPS, INPT, LAPLACE (Laboratoire Plasma et Conversion d'Energie), 118 Route de Narbonne, 31062 Toulouse Cedex 9, France
[2] CORIA, UMR CNRS 6614, Université de Rouen, Site universitaire du Madrillet, BP 12, 76801 Saint-Etienne du Rouvray, France

Abstract. This work is devoted to the calculation of the composition for a monoatomic plasma (argon in the case presented) for which the assumption of thermal equilibrium is not realized. The plasma composition is obtained from a CR model, taking into account free electrons and a great number of electronic levels of Ar atoms and Ar^+ ions. This model is based on a large set of transition probabilities and reaction rate coefficients for radiative processes (spontaneous emission and radiative recombination) and on an extended database of direct and reverse reaction rate coefficients for collisional processes (excitation/de-excitation and ionization/recombination mechanisms). Assuming Maxwellian energy distribution functions for electrons and heavy chemical species, detailed balance equations are determined for all kind of reactions in the frame of the micro reversibility principle. From these balance equations, reverse rate coefficients are calculated as a function of direct reaction rates and of electrons and heavy particles translation temperatures (T_e and T_h respectively). Particular attention is paid to problematic chemical reactions with electrons involved on one side and only heavy species on the other side such as: $Ar + Ar \rightarrow Ar + Ar^+ + e$. The detailed balance relations obtained for ionization/recombination processes demonstrate the non-uniqueness of the multi-temperature Saha-Eggert law (i.e. non-uniqueness of the multi-temperature law of mass action). Multi-temperature argon plasma compositions obtained in the present work exhibit abrupt density variations. These sharp variations are characteristic of the transition between the domination of heavy particle reactions (at low temperature) and the predominance of electron collisions (at high temperature).

1 Introduction

The majority of the theoretical studies concerning electric arcs and thermal plasma processes are carried out assuming local thermodynamic equilibrium (LTE) with the implementation of magneto-hydrodynamic (MHD) models ([1] and references therein).

However, it is now well known that the LTE hypothesis is not valid in some particular areas of the plasma: in the close vicinity of the electrodes (cathode and anode sheaths) and the walls (nozzles of torches or breaking devices) and in the external zones of the arc where the turbulence phenomenon and the pumping of surrounding cold gas play a significant role. The LTE assumption is also uncertain during arc decay or within the plasma column in the case of low power arcs. In this last case, the temperature and the electron number density remain relatively low, even on the axis of the plasma. Thus the energy transfer (through elastic collisions) between the electrons and heavy particles is not efficient enough to preserve the equal distribution of energy between the various chemical species. The consequence is that the electrons have a kinetic temperature T_e higher than that of the heavy species T_h.

To study theoretically this kind of discharge, taking into account the possible occurrence of departures from thermal equilibrium, it is necessary to develop multi temperature MHD models. There are more and more publications in the literature dealing with multi-T fluid models such as the works of Mostaghimi et al. [2], El Morsli and Proulx [3], Tanaka [4], Ye et al. [5] and Al-Mamun et al. [6] concerning respectively argon, air, Ar-N_2, Ar-H_2 and Ar-CO_2-H_2 radio-frequency inductively coupled plasma (ICP) torches, Ghorui et al. [7] for the study of the oxygen flow inside the nozzle of a metal cutting device, Boselli et al. [8] concerning a direct current (DC) welding arc in argon, Trelles et al. [9], Bartosiewicz at al. [10] and Kaminska et al. [11] for the study of a DC plasma torch in argon, Baeva and Uhrlandt [12] and Freton et al. [13] concerning free-burning arcs in argon, Colombo et al. [14]

[b] e-mail: philippe.teulet@laplace.univ-tlse.fr

[a] *Present address*: CNES, 18 Avenue Édouard Belin, 31400 Toulouse, France.

for a 3D transient model of a twin torch system, Park et al. [15] for a DC transferred arc in argon and Benilov and Naidis [16] for the study of a wall-stabilized DC arc discharge.

The implementation of these multi-T models is based upon 2T thermodynamic and transport property databases (as a function of T_e and of the ratio $\theta = T_e/T_h$) and the first and unavoidable step in obtaining these 2T properties is the calculation of the plasma composition. The fundamental theoretical concepts necessary for the calculation of 2T transport coefficients are expounded in the works of Rat [17], Rat et al. [18,19], Devoto [20] and Bonnefoi [21]. 2T thermodynamic and transport property databases are also available for several gases or mixtures such as argon [18,19], lithium [22], N_2 [23,24], O_2 [25], SF_6 [26], N_2-O_2 [27], carbon-oxygen [28], N_2-H_2 [29], argon-helium [30], Ar-H_2 [29,31,32], argon-copper [33] and Ar-H_2-He [34]. These studies are founded upon solid theoretical bases with the exception of the calculation of the composition. Indeed, there is no consensus in the literature and the theory allowing the computation of composition for plasmas in thermal non-equilibrium conditions is not yet clearly established.

The three main methods available in the literature for the calculation of the plasma composition are:

1. The minimization of a thermodynamic function (Gibbs free enthalpy or Helmholtz free energy respectively for a plasma at constant pressure and a plasma at constant volume) [35].
2. The resolution of a non-linear system of equations built with the equation of pressure conservation (or mass density conservation for an isochoric system), the equation of electro-neutrality, one or several equation(s) of mixture proportion conservation and the law of mas action [36].
3. A kinetic or collisional-radiative (CR) model [37,38]. With this kind of approach, the plasma composition is obtained from the resolution of a non-linear system of conservation equations for each electronic level or chemical species. These equations are dependent on the population number densities and on the forward and reverse rate coefficients of the chemical reactions occurring in the plasma.

The three techniques mentioned above are presented for the multi-T case in the review by Rat et al. [39]. They obviously all lead to the same results in the case of thermodynamic equilibrium but they strongly differ in thermal non-equilibrium conditions, depending on the initial calculation assumptions.

The method 1 (minimization of a thermodynamic function) has been used by several authors [40,41] to calculate 2T plasma compositions but we believe that this technique should be used very carefully in thermal nonequilibrium conditions because it is difficult to determine in this case what the accurate thermodynamic function is to minimize. Moreover, there is still a controversy in the literature concerning this technique. On one side, Chen and Han [42] have argued that the Gibbs free enthalpy or the Helmholtz free energy minimization approach is unusable in a 2T-plasma. These authors have claimed that the principle of entropy maximization should be preferred. On the other side, André et al. [43], on the basis of statistical mechanical considerations, have arrived at the exact opposite conclusion.

Concerning the second method based upon a multi-temperature law of mass action, there are many attempts in the literature to generalize the Saha-Eggert equation to two-temperature plasmas. In particular, one can mention:

- The equation proposed by Prigogine [44] and Potapov [45], here given in the case of atomic species:

$$n_e \left(\frac{n_A^+}{n_A}\right)^{\frac{1}{\theta}} = \frac{2 \times Q_{int,A^+}(T_e)}{Q_{int,A}(T_e)} \left(\frac{2\pi m_e k_B T_e}{h^2}\right)^{3/2} \times \exp\left(-\frac{E_{ion}^A}{k_B T_e}\right) \quad (1)$$

  where m_e is the electron mass, k_B the Boltzmann constant, h the Planck constant and E_{ion}^A the ionization energy of the atomic species A. n_e, n_A and n_A^+ are the population number densities of electrons, atoms A and ions A^+ respectively. $Q_{int,A}$ and Q_{int,A^+} are the internal partition functions of A and A^+.
- The 2T Saha-Eggert relation established by Van de Sanden et al. [46] (Eindhoven formulation):

$$n_e \left(\frac{n_A^+}{n_A}\right) = \frac{2 \times Q_{int,A^+}(T_e)}{Q_{int,A}(T_e)} \left(\frac{2\pi m_e k_B T_e}{h^2}\right)^{3/2} \times \exp\left(-\frac{E_{ion}^A}{k_B T_e}\right). \quad (2)$$

  In the case of atomic species, this equation differs from the one of Potapov by the lack of the exponent term $1/\theta$.
- The 2T Saha-Eggert relation in which the internal energy states population and the ionization process are governed by an excitation temperature T_{ex} varying between T_e and T_h:

$$n_e \left(\frac{n_A^+}{n_A}\right) = \frac{2 \times Q_{int,A^+}(T_{ex})}{Q_{int,A}(T_{ex})} \left(\frac{2\pi m_e k_B T_e}{h^2}\right)^{3/2} \times \exp\left(-\frac{E_{ion}^A}{k_B T_{ex}}\right). \quad (3)$$

  Tanaka et al. [47] suggested the estimation of the excitation temperature T_{ex} from the fraction of kinetic energy absorbed by heavy particles due to elastic collisions. A better approach is that of Gleizes et al. [48] in which the excitation temperature is derived from inelastic collisions (electron and heavy particle impact excitation and deexcitation). André et al. [49] also suggested the use of an effective temperature T^* related to chemical species fluxes and depending on T_e, T_h and n_e.

In our point of view, method 2 based upon the law of mass action should be also used very carefully for the calculation of multi-T plasma composition. Indeed, according to Giordano and Capitelli [50] and as is demonstrated in the present paper, the law of mass action is not unique in thermal non-equilibrium conditions. As a consequence, it is impossible to access an accurate 2T-plasma composition from a unique multi-T law of mass action. Even with the use of an excitation temperature, the plasma composition is only roughly estimated. Indeed, the variation of T_{ex} between T_e and T_h cannot be determined accurately because of unavoidable simplifying assumptions for its calculation.

As stated above, the third method to access a multi-T plasma composition is based on a kinetic or CR model. This kind of technique has already been used by several authors to achieve multi-T plasma composition calculation. Research includes: the works of Bacri et al. [51], Kunc and Soon [52] and Pierrot et al. [53] for nitrogen plasmas, the papers of Gomes et al. [54] and Soon and Kunc [55] for oxygen and the works of Laux et al. [56] and Teulet et al. [57] in the case of the air. CR models are also used for the study of atmospheric entry problems [58–62] for their ability to determine particle number densities inside the non-equilibrium reactive hypersonic plasma flow created by the shock layer in front of the heat shield during the entry of a spacecraft into the upper atmosphere. These kinds of works can be classified according to the composition of the studied planetary atmosphere: the Earth (Ar-O_2-N_2) [63–65], Mars (Ar-CO_2-N_2) [65,66] or Titan (CH_4-N_2) [67] for example.

Lastly, it should be noted that several authors have attempted to confront the 3 methods (listed above) allowing the computation of multi-T plasma composition:

- Gibbs free enthalpy minimization vs kinetic model [68];
- Gibbs free enthalpy minimization vs 2T law of mass action [69];
- 2T law of mass action vs kinetic model [70–72].

Unfortunately, these comparisons did not remove the uncertainties and the controversy on the problem of multi-T plasma composition calculation.

In our point of view, the best and most accurate technique to obtain the plasma composition under thermal nonequilibrium conditions is the CR model. Indeed, compared to the two other techniques, this kind of approach allows the avoidance of the simplifying assumptions associated with the internal excitation modes (electronic, vibrational and rotational). On the other hand, CR models are more complex to develop because they require the implementation of an extended and complete cross sections or reaction rate coefficients database for all inelastic collisional processes between the chemical species of the plasma.

In the present work, a detailed CR model taking into account a great number of electronic levels of Ar atoms and Ar^+ ions is proposed to determine the composition of argon plasma in thermal non-equilibrium conditions. In order to obtain an accurate result, the two following points corresponding to basic initial assumptions for the calculation are crucial:

- the dependence of the direct reaction rate coefficients as a function of temperatures T_e and T_h;
- the use of accurate detailed balance relations for the calculation of reverse rate coefficients.

Particular attention is paid to this last point in the present study. For problematic reactions in the case of plasmas generated from a monoatomic gas (such as $Ar + Ar \rightarrow Ar^+ + Ar + e$ for which there are only heavy particles involved in the forward process and electrons and heavy species in the reverse mechanism), accurate detailed balance relations are obtained in the frame of the micro-reversibility principle. From this work we will also demonstrate the non-uniqueness of the multi-temperature Saha-Eggert equation (that is to say the non-uniqueness of the multi-T law of mass action).

2 Model

2.1 Energy diagram

Three types of species are considered in this CR model: Ar atoms, Ar^+ ions and electrons. The energy diagram of argon used in this study is taken directly from the NIST database [73]. Thus, 379 electronic levels have been selected for Ar. Concerning Ar^+, only the first seven electronic levels are considered. Thus, all possible transitions between states until 32.2 eV above the ground state of Ar can then be taken into account: this is compatible with the values considered in the present work for the heavy and electron kinetic temperatures (i.e. T_e and T_h lower than 15 000 K).

Density effects on the ionization potential of energy levels are not considered here. The plasma studied can therefore be assumed as totally ideal.

Each considered electronic level of Ar and Ar^+ can interact through different elementary processes, detailed in the following section.

2.2 Elementary processes

Heavy particle and electron energy distribution functions are assumed to be Maxwellian at the temperature T_h and T_e, respectively. No assumptions are made on the electronic storage mode; the CR model is in fact totally electronically specific. In the following, each rate coefficient is expressed in $m^3 \cdot s^{-1}$ and the temperature is expressed in K.

2.2.1 Radiative processes

Ar and Ar^+ can produce radiation by means of spontaneous emission processes

$$Ar_j \xrightarrow{A_{ji}} Ar_{i<j} + h\nu \tag{4}$$

$$Ar_n^+ \xrightarrow{A_{nm}} Ar_{m<n}^+ + h\nu \tag{5}$$

The Einstein coefficients $A_{ji}(s^{-1})$ from the NIST database [73] have been directly used. In total, 423 lines have been taken into account for argon, and 3 lines for Ar^+.

Radiative recombination processes of the type

$$Ar_m^+ + e^- \xrightarrow{k^{RR}_{m\to i}(T_e)} Ar_i + h\nu \tag{6}$$

have also been taken into account. The cross-sections due to Zel'dovich and Raizer [74], assuming a hydrogen-like behavior for the atom Ar on its excited state i after recombination, have been used and integrated under the Maxwell-Boltzmann distribution for the kinetic energy ε of electrons. The rate coefficient for radiative recombination is finally given by [64]

$$k^{RR}_{m\to i}(T_e) = \sqrt{\frac{8k_BT_e}{\pi m_e}}\frac{32\pi a_0^2}{3\sqrt{3}\times 137^3}\left(\frac{E^H_{ion}}{k_BT_e}\right)^2 \times \left(\frac{E_m - E_i}{E_m}\right)^{3/2}\xi_1(a)\times e^a \tag{7}$$

where a_0 is the first Bohr radius, E^H_{ion} the ionization energy of the hydrogen atom. E_i and E_m are the energy of the electronic levels i and m of Ar and Ar^+ respectively. $a = (E_m - E_i)/k_BT_e$ and $\xi_p(a)$ is the exponential integral of the order p:

$$\xi_p(a) = \int_1^\infty \frac{e^{-ay}}{y^p}dy. \tag{8}$$

Note: In this work, the Einstein coefficients A_{ji} for spontaneous emission and the radiative recombination rate coefficients $k^{RR}_{m\to i}(T_e)$ are multiplied by an escape factor Λ (dimensionless parameter). This escape factor will be fixed successively to its two extreme values: $\Lambda = 1$ (optically thin plasma) and $\Lambda = 0$ (optically thick plasma) in order to evaluate the influence of radiative processes on the plasma composition.

2.2.2 Electron impact

Under electron impact, Ar_i can be excited or ionized by the elementary processes

$$Ar_i + e^- \xrightarrow{k_{exc}} Ar_{j>i} + e^- \tag{9}$$

$$Ar_i + e^- \xrightarrow{k_i} Ar_m^+ + 2e^- \tag{10}$$

and Ar_m^+ can be excited according to the elementary process

$$Ar_m^+ + e^- \xrightarrow{k_{exc}} Ar_{n>m}^+ + e^-. \tag{11}$$

Using the Drawin's cross sections [75], an analytical form for the rate coefficient has been obtained for each type of transition:

$$k^A_{i\to j}(T_e) = \sqrt{\frac{8k_BT_e}{\pi m_e}}4\pi a_0^2a^2\alpha^A\left(\frac{E^H_{ion}}{E_j - E_i}\right)^2\left[\ln\left(\frac{5}{4}\beta^A\right)\times\left(\frac{e^{-a}}{a} - \xi_1(a)\right) + \frac{\xi_1(a)}{a} - G_2(a)\right] \tag{12}$$

for the excitation of an optically allowed transition,

$$k^P_{i\to j}(T_e) = \sqrt{\frac{8k_BT_e}{\pi m_e}}4\pi a_0^2a^2\alpha^P\left[\frac{e^{-a}}{a} - \xi_1(a)\right] \tag{13}$$

for the excitation of a parity forbidden transition,

$$k^S_{i\to j}(T_e) = \sqrt{\frac{8k_BT_e}{\pi m_e}}4\pi a_0^2a^2\alpha^S\left[\xi_2(a) - \xi_4(a)\right] \tag{14}$$

for the excitation of a spin forbidden transition,

$$k^+_{i\to m}(T_e) = \sqrt{\frac{8k_BT_e}{\pi m_e}}4\pi a_0^2a^2\alpha^+\left(\frac{E^H_{ion}}{E_m - E_i}\right)^2\left[\ln\left(\frac{5}{4}\beta^+\right)\times\left(\frac{e^{-a}}{a} - \xi_1(a)\right) + \frac{\xi_1(a)}{a} - G_2(a)\right] \tag{15}$$

for an ionization process. The parameters $\alpha^{A,P,S,+}$and $\beta^{A,+}$ are chosen as mean values resulting from comparisons with available experimental cross sections [76]. $G_p(a)$ is the generalized exponential integral of the order p:

$$G_p(a) = \frac{1}{(p-1)!}\int_1^\infty \frac{e^{-ay}}{y}\left[\ln(y)\right]^{p-1}dy. \tag{16}$$

2.2.3 Heavy particle impact

Concerning the electronic excitation and ionization by heavy particle impact, such as

$$Ar_i + \left(\frac{\sum Ar_i}{\sum Ar_m^+}\right) \xrightarrow{k_{exc}} Ar_{j>i} + \left(\frac{\sum Ar_i}{\sum Ar_m^+}\right) \tag{17}$$

$$Ar_m^+ + \left(\frac{\sum Ar_i}{\sum Ar_m^+}\right) \xrightarrow{k_{exc}} Ar_{n>m}^+ + \left(\frac{\sum Ar_i}{\sum Ar_m^+}\right) \tag{18}$$

$$Ar_i + \left(\frac{\sum Ar_i}{\sum Ar_m^+}\right) \xrightarrow{k_i} Ar_m^+ + \left(\frac{\sum Ar_i}{\sum Ar_m^+}\right) + e^-. \tag{19}$$

Once again the cross-sections proposed by Drawin and Emard [77] have been selected

$$\sigma^A_{i\to j}(\varepsilon) = 4\pi a_0^2\left(\frac{E^H_{ion}}{E_j - E_i}\right)^2\frac{m_{Ar}}{m_H}\xi_i^2 f_{ij}\frac{2m_e}{m_{Ar}+m_e} \times \frac{\left(\frac{\varepsilon}{E_j - E_i} - 1\right)}{\left[1 + \left(\frac{2m_e}{m_{Ar}+m_e}\right)\left(\frac{\varepsilon}{E_j - E_i} - 1\right)\right]^2} \tag{20}$$

for the excitation of optically allowed transitions,

$$\sigma^{+}_{i\to m}(\varepsilon) = 4\pi a_0^2 \left(\frac{E^H_{ion}}{E_m - E_i}\right)^2 \frac{m_{Ar}}{m_H}\xi_i^2 \frac{2m_e}{m_{Ar}+m_e} \times \frac{\left(\frac{\varepsilon}{E_m - E_i} - 1\right)}{\left[1 + \left(\frac{2m_e}{m_{Ar}+m_e}\right)\left(\frac{\varepsilon}{E_m - E_i} - 1\right)\right]^2} \quad (21)$$

for ionization.

In equations (20) and (21) m_{Ar} and m_H are the masses of argon and hydrogen atoms, ε is the relative kinetic energy of incident particles, ξ_i is the number of optical electrons and f_{ij} the absorption oscillator strength, such as [78]:

$$f_{ij} = \frac{m_e c \varepsilon_0}{2\pi e^2}\frac{g_j}{g_i}\lambda_{ji}^2 A_{ji} \quad (22)$$

where c is the speed of light, e is the elementary charge, ε_0 is the vacuum permittivity, λ_{ji} is the wavelength corresponding to the transition, and g_j and g_i are the degeneracies of the electronic levels j and i.

It should be noted that cross sections $\sigma^{A}_{i\to j}(\varepsilon)$ and $\sigma^{+}_{i\to m}(\varepsilon)$ (respectively for excitation of optically allowed transitions and for ionization) are very close to one another (they only differ by the lack of the oscillator strength f_{ij} for ionization). Indeed, a transition to the continuum (ionization) is considered as optically allowed since the electron produced by the ionization process is not bound. Thus, the two calculation formulations proposed by Drawin and Emard are quasi identical.

The rate coefficients for these processes are obtained by the integration of the cross-sections with the assumption of a Maxwellian energy distribution function for heavy particles:

$$k^{A \text{ or } +}_{i\to j \text{ or } m}(T_h) = \sqrt{\frac{8k_B T_h}{\pi\mu}} \int_0^{+\infty} y e^{-y}\sigma(y)dy \quad (23)$$

where $y = \varepsilon/k_B T_h$ and μ is the reduced mass of the collision partners. These rate coefficients are then interpolated under the modified Arrhenius law:

$$k^{A \text{ or } +}_{i\to j \text{ or } m}(T_h) = A(i,j \text{ or } m) T_h^{\alpha(i,j \text{ or } m)} \times e^{-B(i,j \text{ or } m)/T_h}. \quad (24)$$

Note: For heavy particle impact forbidden transitions, there is no cross section formulation proposed by Drawin and Emard and, to our knowledge, no form proposed in the literature. As a consequence, for forbidden transitions, we have used the same formulation as for allowed transitions, i.e. relation (20), provided that an oscillator strength for the considered forbidden transition is available in the NIST database [73]. Other heavy particle impact forbidden transitions are not taken into consideration.

2.2.4 Backward rate coefficients

For the atom/ion excitation, the backward rate coefficient is directly calculated by the 2T-Boltzmann equilibrium law:

$$\frac{k_{Forward}}{k_{Backward}} = \frac{g_j}{g_i}\exp\left(-\frac{E_j - E_i}{k_B T_h}\right) \quad (25)$$

if the collisional partners are the heavies,

$$\frac{k_{Forward}}{k_{Backward}} = \frac{g_j}{g_i}\exp\left(-\frac{E_j - E_i}{k_B T_e}\right) \quad (26)$$

if the collisional partners are the electrons.

Concerning ionization, it is first necessary to consider carefully the heavy particle impact process (i.e. with only heavy species in the forward mechanism but heavy particles and electrons in the reverse mechanism). Indeed, for this ionization reaction, the detailed balance relation allowing the calculation of the reverse rate coefficient is not obvious. This ionization process is expressed below in its more general form:

$$A(\vec{v}_A) + S(\vec{v}_S) \underset{\sigma_R}{\overset{\sigma_I}{\longleftrightarrow}} A^+(\vec{v}_+) + e^-(\vec{v}_e) + S(\vec{v}_{S'}) \quad (27)$$

where $\vec{v}_X$ are the various speeds of each chemical species X involved in the collisional process. σ_I and σ_R are respectively the cross sections for ionization (direct reaction) and recombination (reverse mechanism). From these cross sections, it is possible to calculate the rate coefficients for ionization k_I and recombination k_R. This will be done in the following sections.

2.2.4.1 Rate coefficient for ionization k_I

According to Hochstim [79], the ionization rate coefficient k_I for reaction (27) is given by:

$$k_I = \int \sigma_I(|\vec{v}_A - \vec{v}_S|) d^3w_+ d^3w_{S'} |\vec{v}_A - \vec{v}_S| \times f_A(\vec{v}_A) f_S(\vec{v}_S) d^3v_A d^3v_S \quad (28)$$

where $\vec{w}_+ = \vec{v}_e - \vec{v}_+$ and $\vec{w}_{S'} = \vec{v}_e - \vec{v}_{S'}$ are the relative velocities between the electron and the ion A^+ and between the electron and the neutral particle S. Under thermal nonequilibrium conditions ($T_A \neq T_S$) and with the assumption that the velocity distribution functions f_A and f_S for chemical species A and S are Maxwellian, the ionization rate coefficient k_I is only dependent on the kinetic temperatures T_A and T_S of the collision partners A and S. Relation (28) is finally rewritten as:

$$k_I = \left(\frac{m_A}{2\pi k_B T_A}\right)^{3/2}\left(\frac{m_S}{2\pi k_B T_S}\right)^{3/2} \times \int \sigma_I(|\vec{v}_A - \vec{v}_S|) d^3w_+ d^3w_{S'} |\vec{v}_A - \vec{v}_S| \times \exp\left(-\frac{m_A v_A^2}{2k_B T_A}\right)\exp\left(-\frac{m_S v_S^2}{2k_B T_S}\right) d^3v_A d^3v_S \quad (29)$$

where m_A and m_S are the masses of species A and S.

Let us assume that $q_A = m_A/T_A$ and $q_S = m_S/T_S$, and that the relative velocity between the collision partners A and S is $\vec{w} = \vec{v}_A - \vec{v}_S$. Let us now introduce a fictitious velocity:

$$\vec{W}_{AS} = \frac{q_A\vec{v}_A + q_S\vec{v}_S}{q_A + q_S}. \tag{30}$$

It is then possible to write:

$$\begin{aligned}\frac{m_A v_A^2}{T_A} + \frac{m_S v_S^2}{T_S} &= q_A v_A^2 + q_S v_S^2 \\ &= \theta_{AS} W_{AS}^2 + \frac{q_A q_S}{q_A + q_S} w^2\end{aligned} \tag{31}$$

with $\theta_{AS} = q_A + q_S$.

The introduction of equation (31) in relation (29) gives:

$$\begin{aligned}k_I = &\left(\frac{m_A}{2\pi k_B T_A}\right)^{3/2}\left(\frac{m_S}{2\pi k_B T_S}\right)^{3/2} \\ &\times \int \sigma_I(w) d^3w_+ d^3w_{S'} w \exp\left(-\frac{\theta_{AS} w_{AS}^2}{2k_B}\right) \\ &\times \exp\left(-\frac{q_A q_S}{q_A + q_S} w^2/2k_B\right) d^3v_A d^3v_S.\end{aligned} \tag{32}$$

A variable change is thus realized: $(\vec{v}_A, \vec{v}_S) \rightarrow (\vec{W}_{AS}, \vec{w})$. This variable change is unitary (its Jacobian module is equal to 1). Thus $d^3v_A d^3v_S = d^3W_{AS} d^3w$ and equation (32) becomes:

$$\begin{aligned}k_I = &\left(\frac{m_A}{2\pi k_B T_A}\right)^{3/2}\left(\frac{m_S}{2\pi k_B T_S}\right)^{3/2} \\ &\times \int \exp\left(-\frac{\theta_{AS} w_{AS}^2}{2k_B}\right) d^3W_{AS} \\ &\times \int \sigma_I(w) d^3w_+ d^3w_{S'} w \\ &\times \exp\left(-\frac{q_A q_S}{q_A + q_S} w^2/2k_B\right) d^3w.\end{aligned} \tag{33}$$

Integration over W_{AS} leads to:

$$\begin{aligned}\int \exp\left(-\frac{\theta_{AS} w_{AS}^2}{2k_B}\right) d^3W_{AS} &\equiv 4\pi \int_0^\infty W_{AS}^2 \\ &\times \exp\left(-\frac{\theta_{AS} w_{AS}^2}{2k_B}\right) dW_{AS} \\ &= \left(\frac{2\pi k_B}{\theta_{AS}}\right)^{3/2}.\end{aligned} \tag{34}$$

The introduction of relation (34) in equation (33) gives the final expression of the ionization rate coefficient:

$$\begin{aligned}k_I = &\left(\frac{m_A m_S}{2\pi k_B T_A T_S \theta_{AS}}\right)^{3/2} \int \sigma_I(w) d^3w_+ d^3w_{S'} w \\ &\times \exp\left(-\frac{q_A q_S}{q_A + q_S} w^2/2k_B\right) d^3w.\end{aligned} \tag{35}$$

2.2.4.2 Rate coefficient for recombination k_R

The definition of the recombination rate coefficient k_R for reaction (27) is:

$$\begin{aligned}k_R = &\int \sigma_R(\vec{v}_e - \vec{v}_+, \vec{v}_e - \vec{v}_{S'}) d^3w |\vec{v}_e - \vec{v}_+||\vec{v}_e - \vec{v}_{S'}| \\ &\times f_+(\vec{v}_+) f_e(\vec{v}_e) f_{S'}(\vec{v}_{S'}) d^3v_+ d^3v_e d^3v_{S'}.\end{aligned} \tag{36}$$

The energy distribution functions f_+, f_e and $f_{S'}$ of the chemical species A^+, e^- and S are assumed to be Maxwellian. The reaction rate k_R is thus only dependent on the kinetic temperatures T_+, T_e and $T_{S'}$ of the three collision partners. In a similar way to the case of ionization, if it is assumed that $q_+ = m_+/T_+$, $q_e = m_e/T_e$, $q_{S'} = m_S/T_{S'}$ and $\theta_{+eS'} = q_+ + q_e + q_{S'}$, and the fictitious velocity $\vec{W}_{+eS'}$ is introduced:

$$\vec{W}_{+eS'} = \frac{q_+\vec{v}_+ + q_e\vec{v}_e + q_{S'}\vec{v}_{S'}}{q_+ + q_e + q_{S'}}. \tag{37}$$

It is then possible to write:

$$\begin{aligned}&\frac{m_+ v_+^2}{T_+} + \frac{m_e v_e^2}{T_e} + \frac{m_{S'} v_{S'}^2}{T_{S'}} \\ &= q_+ v_+^2 + q_e v_e^2 + q_{S'} v_{S'}^2 \\ &= \theta_{+eS'} W_{+eS'}^2 \\ &\quad + \frac{q_+ q_{S'} (\vec{w}_+ - \vec{w}_{S'})^2 + q_e(q_+ w_+^2 + q_{S'} w_{S'}^2)}{q_+ + q_e + q_{S'}}\end{aligned} \tag{38}$$

As $q_e \ll q_+$ and $q_e \ll q_{S'}$ (because of the respective masses of the collision partners e, A^+ and S), it is possible to simplify equation (38):

$$\begin{aligned}&\frac{m_+ v_+^2}{T_+} + \frac{m_e v_e^2}{T_e} + \frac{m_{S'} v_{S'}^2}{T_{S'}} \\ &= q_+ v_+^2 + q_e v_e^2 + q_{S'} v_{S'}^2 \\ &= \theta_{+eS'} W_{+eS'}^2 \\ &\quad + \frac{q_+(q_{S'} + q_e) w_+^2 + q_{S'}(q_+ + q_e) w_{S'}^2 - 2q_+ q_{S'} \vec{w}_+ \vec{w}_{S'}}{q_+ + q_e + q_{S'}} \\ &\cong \theta_{+eS'} W_{+eS'}^2 + \frac{q_+ q_{S'} w_+^2 + q_{S'} q_+ w_{S'}^2 - 2q_+ q_{S'} \vec{w}_+ \vec{w}_{S'}}{q_+ + q_{S'}} \\ &\cong \theta_{+eS'} W_{+eS'}^2 + \frac{q_+ q_{S'} (\vec{w}_+ - \vec{w}_{S'})^2}{q_+ + q_{S'}}\end{aligned} \tag{39}$$

$$\frac{k_I}{k_R} = \left(\frac{m_A m_S}{2\pi k_B T_A T_S \theta_{AS}} \frac{(2\pi k_B)^2 T_+ T_e T_{S'} \theta_{+eS'}}{m_+ m_e m_{S'}}\right)^{3/2} \times \frac{\int \sigma_I(w) d^3w_+ d^3w_{S'} w \exp\left(-\frac{q_A q_S}{q_A+q_S} w^2/2k_B\right) d^3w}{\int \sigma_R(\vec{w}_+,\vec{w}_{S'}) d^3w \cdot w_+ w_{S'} \exp\left(-\frac{q_+ q_{S'}(\vec{w}_+ - \vec{w}_{S'})^2}{q_+ + q_{S'}}/2k_B\right) d^3w_+ d^3w_{S'}} \quad (42)$$

The change of variable $(\vec{v}_+, \vec{v}_e, \vec{v}_{S'}) \rightarrow (\vec{W}_{+eS'}, \vec{w}_+, \vec{w}_{S'})$ is also unitary, leading to $d^3v_+ d^3v_e d^3v_{S'} = d^3W_{+eS'} d^3w_+ d^3w_{S'}$. The recombination rate coefficient k_R given by equation (36) can be rewritten as:

$$k_R = \left(\frac{m_+ m_e m_{S'}}{(2\pi k_B)^3 T_+ T_e T_{S'}}\right)^{3/2} \int \sigma_R(\vec{w}_+,\vec{w}_{S'}) d^3w \cdot w_+ w_{S'} \times \exp\left(-\frac{\theta_{+eS'} W_{+eS'}^2}{2k_B}\right) \times \exp\left(-\frac{q_+ q_{S'}(\vec{w}_+ - \vec{w}_{S'})^2}{q_+ + q_{S'}}/2k_B\right) \times d^3W_{+eS'} d^3w_+ d^3w_{S'}. \quad (40)$$

Integration over $W_{+eS'}$ (as in equation (34) leads to the final expression of the recombination rate coefficient k_R:

$$k_R = \left(\frac{m_+ m_e m_{S'}}{(2\pi k_B)^2 T_+ T_e T_{S'} \theta_{+eS'}}\right)^{3/2} \times \int \sigma_R(\vec{w}_+,\vec{w}_{S'}) d^3w \cdot w_+ w_{S'} \times \exp\left(-\frac{q_+ q_{S'}(\vec{w}_+ - \vec{w}_{S'})^2}{q_+ + q_{S'}}/2k_B\right) \times d^3w_+ d^3w_{S'}. \quad (41)$$

Note: As expected, this is the slowest process i.e. the interaction between heavy species A^+ and S ($\vec{w}_+ - \vec{w}_{S'} = \vec{v}_{S'} - \vec{v}_+$) which is controlling the recombination reaction rate as shown by relation (41).

2.2.4.3 Calculation of the ratio k_I/k_R

From equations (35) and (41), it is possible to deduce the ratio k_I/k_R:

See equation (42) above.

With the introduction of the fundamental principle of energy conservation in the frame of the center of mass system of the collision partners involved in reaction (27):

$$E_{AS} = \frac{1}{2} m_A (\vec{v}_A - \vec{v}_{CM})^2 + \frac{1}{2} m_S (\vec{v}_S - \vec{v}_{CM})^2$$
$$E_{AS} = \frac{1}{2} \frac{m_A m_S}{m_A + m_S} w^2$$
$$E_{AS} = \frac{1}{2} m_e (\vec{v}_e - \vec{v}_{CM})^2 + \frac{1}{2} m_+ (\vec{v}_+ - \vec{v}_{CM})^2 + \frac{1}{2} m_{S'} (\vec{v}_{S'} - \vec{v}_{CM})^2 + E_{ion}$$
$$E_{AS} = \frac{1}{2} \frac{m_+ m_{S'}}{m_+ + m_{S'}} (\vec{w}_+ - \vec{w}_{S'})^2 + E_{ion}$$

With the assumption $m_e \ll m_+$ and $m_e \ll m_{S'}$

$$E_{AS} = E_{+eS'} + E_{ion} \quad (43)$$

where E_{ion} is the ionization energy of species A and $\vec{v}_{CM}$ is the velocity of the center of mass given by:

$$\vec{v}_{CM} = \frac{m_A \vec{v}_A + m_S \vec{v}_S}{m_A + m_S} = \frac{m_+ \vec{v}_+ + m_e \vec{v}_e + m_{S'} \vec{v}_{S'}}{m_+ + m_e + m_{S'}}. \quad (44)$$

In order to simplify the calculation, it will now be considered that all the heavy chemical species have the same kinetic temperature: $T_A = T_S = T_+ = T_{S'} = T_h$. Moreover, as $q_e \ll q_+$ and $q_e \ll q_{S'}$, we have $\theta_{+eS'} = \theta_{AS}$ and the two following relations can be written:

$$\frac{q_A q_S}{q_A + q_S} = \frac{m_A m_S}{m_A + m_S} \frac{1}{T_h} = 2\frac{E_{AS}}{w^2} \frac{1}{T_h} = 2\frac{E_{+eS'} + E_{ion}}{w^2} \frac{1}{T_h} \quad (45)$$

$$\frac{q_+ q_{S'}}{q_+ + q_{S'}} = \frac{m_+ m_{S'}}{m_+ + m_{S'}} \frac{1}{T_h} = 2\frac{E_{+eS'}}{(\vec{w}_+ - \vec{w}_{S'})^2} \frac{1}{T_h}. \quad (46)$$

From equations (45) and (46), the ratio (42) is rewritten as:

See equation (47) next page.

Considering the ratio of the integrals in equation (47):

$$R = \frac{\int \sigma_I(w) d^3w_+ d^3w_{S'} w \exp\left(-\frac{E_{+eS'}}{k_B T_h}\right) d^3w}{\int \sigma_R(\vec{w}_+,\vec{w}_{S'}) d^3w \cdot w_+ w_{S'} \exp\left(-\frac{E_{+eS'}}{k_B T_h}\right) d^3w_+ d^3w_{S'}}. \quad (48)$$

To simplify this last equation, the fundamental principle of micro-reversibity is introduced. According to Oxenius [80], it is possible to write:

$$\sigma_I(w) \cdot w = \sigma_R(\vec{w}_+,\vec{w}_{S'}) \cdot w_+ w_{S'} \frac{g_e g_+}{g_A} \left(\frac{m_e}{h}\right)^3 \quad (49)$$

$$\frac{k_I}{k_R} = \left(\frac{2\pi k_B T_e}{m_e}\right)^{3/2} \frac{\exp\left(-\frac{E_{ion}}{k_B T_h}\right) \int \sigma_I(w) d^3w_+ d^3w_{S'} w \exp\left(-\frac{E_{+eS'}}{k_B T_h}\right) d^3w}{\int \sigma_R(\vec{w}_+,\vec{w}_{S'}) d^3w \cdot w_+ w_{S'} \exp\left(-\frac{E_{+eS'}}{k_B T_h}\right) d^3w_+ d^3w_{S'}} \tag{47}$$

where g_+ and g_A are the degeneracies of the electronic levels of the ion A^+ and the neutral particle A ($g_e = 2$ for electrons). As a consequence:

$$\begin{aligned}
&\sigma_I(w) \cdot w \cdot d^3w_+ d^3w_{S'} \exp\left(-\frac{E_{+eS'}}{k_B T_h}\right) d^3w \\
&= \sigma_R(\vec{w}_+,\vec{w}_{S'}) \cdot w_+ w_{S'} \frac{g_e g_+}{g_A} \left(\frac{m_e}{h}\right)^3 d^3w_+ d^3w_{S'} \\
&\quad \cdot \exp\left(-\frac{E_{+eS'}}{k_B T_h}\right) d^3w.
\end{aligned} \tag{50}$$

The ratio R given by relation (48) finally reduces to:

$$R = \frac{g_e g_+}{g_A} \left(\frac{m_e}{h}\right)^3. \tag{51}$$

It can be noted that R is not dependent on temperature. The ultimate expression of the ratio of ionization and recombination reaction rate coefficients, i.e. equation (47), is given by:

$$\frac{k_I}{k_R} = \frac{g_e g_+}{g_A} \left(\frac{2\pi m_e k_B T_e}{h^2}\right)^{3/2} \exp\left(-\frac{E_{ion}}{k_B T_h}\right). \tag{52}$$

As the ionization rate coefficient k_I is only dependent on T_h, it has been demonstrated that the reverse recombination rate k_R depends on the two temperatures T_e and T_h according to the detailed balance relation (52).

Important note: The detailed balance relation (52) for reaction (27) agrees with the work of Collins [81]. Indeed, this author has established the same detailed balance relation for ionization/recombination in the case of low temperature plasmas ($T < 5000\,\mathrm{K}$, i.e. in the case where ionization is dominated by the heavy particle impact process) on the basis of the experimental work of Bates and Khare [82].

If the same work is done on the direct and reverse rate coefficients k_I and k_R for the other ionization process (i.e. by electron impact: $A + e^- \leftrightarrow A^+ + e^- + e^-$) occurring in the plasma, the following detailed balance relation, only dependent on the electron temperature, is clearly obtained:

$$\frac{k_I}{k_R} = \frac{g_e g_+}{g_A} \left(\frac{2\pi m_e k_B T_e}{h^2}\right)^{3/2} \exp\left(-\frac{E_{ion}}{k_B T_e}\right). \tag{53}$$

Relations (52) and (53) are two Saha-like equations and they do not depend on the same temperatures. This result demonstrates the non-uniqueness of the Saha-Eggert equation in the case of multi-temperature plasmas (and consequently the non-uniqueness of the law of mass action as the Saha law is only a particular case of the law of mass action). In thermal nonequilibrium conditions, there are non-identical expressions of the multi-T Saha law depending on the considered ionization process. Thus it is not possible to describe rigorously multi-T plasmas with a unique expression of a multi-T law of mass action.

This non-uniqueness of the 2T-Saha law was already supported by Giordano and Capitelli [50] on the basis of thermodynamic considerations (second law of thermodynamics and axiomatic thermodynamics).

2.3 Composition calculation procedure

In this part, the procedure used to determine the Ar, Ar^+ and e^- mixture composition in thermal nonequilibrium conditions ($T_h \neq T_e$) is presented. This composition is calculated at steady state obtained after the temporal relaxation of the mixture using a CR model.

Step 1. Initial thermodynamic conditions

The pressure P, the heavy particle temperature T_h and the electron temperature T_e are chosen. Then the Ar total density n_{Ar}, and the electron density n_e (equal to the Ar^+ total density due to the electroneutrality, i.e. $n_e = n_{Ar^+}$) are driven by the pressure conservation equation

$$P = (n_{\mathrm{Ar}} + n_{Ar^+})\, k_B T_h + n_e k_B T_e. \tag{54}$$

The role of the following steps is to determine the densities involved in the latter equation at steady state.

Step 2. Nonsteady-state initial composition

The composition is initially chosen so that a steady state cannot be obtained with this composition under the values chosen for T_h, T_e and P. Typically, if $n_e < n_e^{SS}$ (superscript SS means steady-state) the mixture will ionize and if $n_e > n_e^{SS}$, the mixture will recombine.

Note that the distributions of the excited states of Ar and Ar^+ are initially chosen in order that they follow a Boltzmann distribution at an arbitrary excitation temperature T_{ex}.

Step 3. Time evolution of the mixture

Since each forward elementary process is not rigorously counterbalanced by the corresponding backward elementary process, owing to the chosen initial composition and the thermal nonequilibrium conditions, the mixture evolves. Its composition tends toward a steady composition different from that initially chosen. The resulting evolution is driven by the different rate coefficients presented in the above sections. They lead to non-zero CR terms in the balance equation of the number of each atom or ion Ar_i or Ar_i^+ contained in a volume $V(t)$. This volume

$$\frac{1}{V(t)}\frac{d}{dt}\begin{pmatrix} \mathrm{Ar}_1 \\ \vdots \\ \vdots \\ \mathrm{Ar}_{i_{\max}} \\ \mathrm{Ar}_1^+ \\ \vdots \\ \vdots \\ \mathrm{Ar}_{m_{\max}}^+ \\ e^- \end{pmatrix} = \begin{pmatrix} \left[\overset{\bullet}{\mathrm{Ar}}_1\right]_C + \left[\overset{\bullet}{\mathrm{Ar}}_1\right]_R \\ \vdots \\ \vdots \\ \left[\overset{\bullet}{\mathrm{Ar}}_{i_{\max}}\right]_C + \left[\overset{\bullet}{\mathrm{Ar}}_{i_{\max}}\right]_R \\ \left[\overset{\bullet}{\mathrm{Ar}}_1^+\right]_C + \left[\overset{\bullet}{\mathrm{Ar}}_1^+\right]_R \\ \vdots \\ \vdots \\ \left[\overset{\bullet}{\mathrm{Ar}}_{m_{\max}}^+\right]_C + \left[\overset{\bullet}{\mathrm{Ar}}_{m_{\max}}^+\right]_R \\ \left[\overset{\bullet}{e}^-\right]_C + \left[\overset{\bullet}{e}^-\right]_R \end{pmatrix} \tag{55}$$

evolves in time in order to keep the pressure P constant along the calculation since the mixture can ionize or recombine.

Due to the total number of species and electronic states considered in the CR model, the set of balance equations can be written as the following system of 387 nonlinear coupled ordinary differential equations:

See equation (55) above.

In the system of equation (55), e^-, Ar_i, Ar_m^+ represent the number of electrons, the number of atoms in level i and the number of ions in state m respectively. $\left[\overset{\bullet}{X}_i\right]_C$ are the source terms of each electronic level i due to collisional processes. These source terms depend on the forward and backward rate coefficients for excitation and ionization reactions (presented in Sects. 2.2.2 and 2.2.3) and on the atomic $[Ar_i] = Ar_i/V(t)$, ionic $[Ar_i^+] = Ar_i^+/V(t)$ and electron $[e^-] = e^-/V(t)$ population number densities. The other source terms $\left[\overset{\bullet}{X}_i\right]_R$ are associated with radiative processes. They also depend on the population number densities, and on the Einstein coefficients and the radiative recombination rate coefficients (cf. Sect. 2.2.1).

The DVODE library [83] especially dedicated to stiff problems is implemented to solve the system of equation (55).

Step 4. Steady state

The steady state is finally obtained after a relaxation time that depends on the values of P, T_h and T_e initially chosen.

3 Results and discussion

As stated in Section 2.3 (step 2), two kinds of non-steady state initial densities are assumed:

- An initial unsteady composition with $n_e < n_e^{SS}$ for each considered value of T_e, T_h and P. During the relaxation time, the mixture evolves with an increase of the electron number density (i.e. the mixture ionizes) to finally reach a steady state. Results obtained with this computation procedure are called "ionization" results in the continuation of this paper.
- An initial unsteady composition with $n_e > n_e^{SS}$. In this case, the mixture recombines (decrease of the electron number density as the mixture evolves). Thus, these results are called "recombination" results in the rest of this work.

When the steady-state is reached, the total population number densities of Ar and Ar^+ are simply obtained with the sum of the population number densities of the electronic levels:

$$n_{\mathrm{Ar}} = \sum_{i}^{i_{\max}} n_{\mathrm{Ar}}(i) \tag{56}$$

$$n_{\mathrm{Ar}}^+ = \sum_{m}^{m_{\max}} n_{\mathrm{Ar}}^+(m). \tag{57}$$

For an optically thick plasma ($\Lambda = 0$), i.e. radiative processes removed from the system of equation (55), the results obtained with the ionization and recombination procedures are presented in Figures 1 and 2 for two non-thermal equilibrium conditions, $\theta = T_e/T_h = 2$ and $\theta = 5$ respectively. For a better visualization of the influence of the ratio θ, these results are also given in Figures 3 and 4 for ionization and recombination respectively, with the two values of θ (2 and 5) in each case.

From these results (Figs. 1–4) the following points should be emphasized:

1. Abrupt transitions in the population number densities of electrons and Ar^+ are clearly observable in all cases.

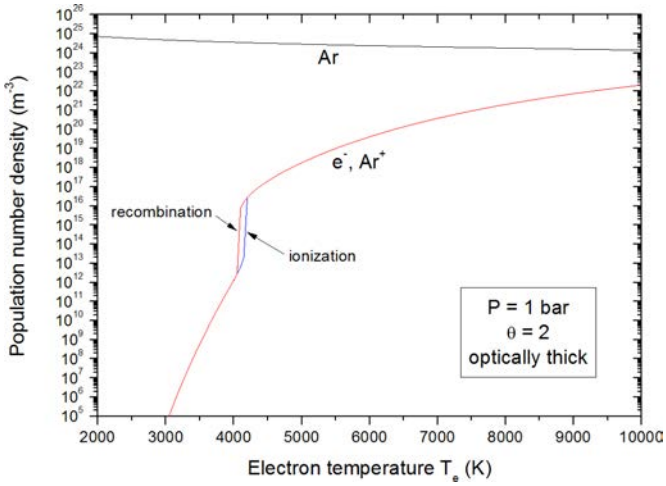

Fig. 1. Argon plasma composition ($\theta = 2$, optically thick).

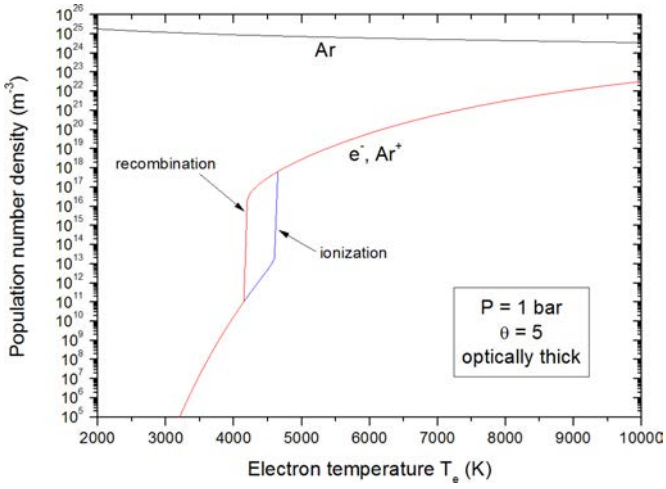

Fig. 2. Argon plasma composition ($\theta = 5$, optically thick).

2. For a given value of the ratio θ, these sharp transitions do not occur at the same electron temperature for ionization and recombination results (cf. Figs. 1 and 2), leading to the formation of a "hysteresis". These severe transitions happen at:
   - $T_e = 4200\,\mathrm{K}$ for $\theta = 2$, ionization case
   - $T_e = 4050\,\mathrm{K}$ for $\theta = 2$, recombination case
   - $T_e = 4650\,\mathrm{K}$ for $\theta = 5$, ionization case
   - $T_e = 4150\,\mathrm{K}$ for $\theta = 5$, recombination case.

From point 2 above (i.e. transitions for ionization and recombination at different electron temperatures for a given value of θ), it is evident that there is not a single solution for the 2T plasma composition in the temperature range corresponding to the hysteresis. Indeed, population densities of electrons and ions are different in this temperature interval in the case of the ionization procedure and for the recombination case.

The temperature range corresponding to abrupt population number density modifications (i.e. the hysteresis area: $4050\,\mathrm{K} < T_e < 4200\,\mathrm{K}$ for $\theta = 2$ and $4150\,\mathrm{K} < T_e < 4650\,\mathrm{K}$ for $\theta = 5$) corresponds to the

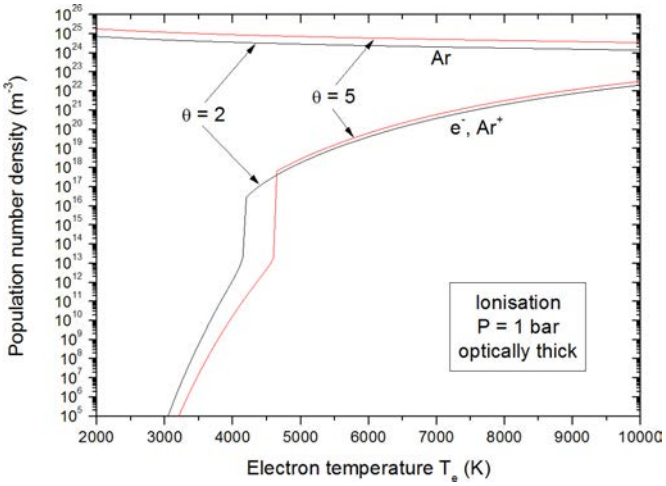

Fig. 3. Argon plasma composition (optically thick, ionization case).

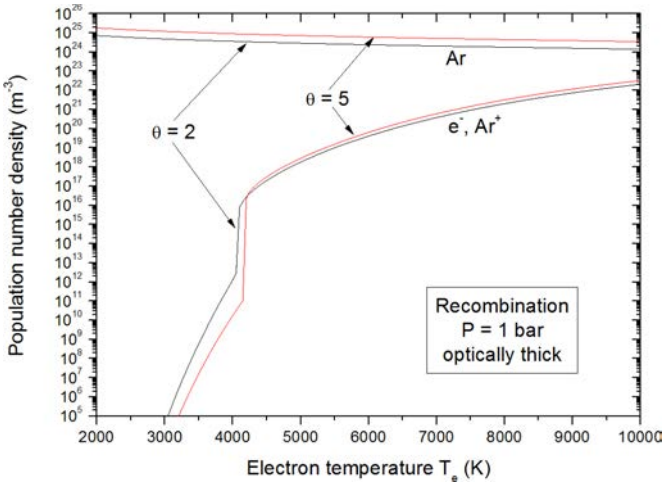

Fig. 4. Argon plasma composition (optically thick, recombination case).

transition between the domination of the heavy particle reactions (at low temperature) and the predominance of the electron collisions (at high temperature). In this temperature region, there is strong competition between the two ionization/recombination processes for creation/disappearance of electrons and ions:

$$\mathrm{Ar}_i + e^- \longrightarrow \mathrm{Ar}_m^+ + 2e^- \tag{58}$$

$$\mathrm{Ar}_i + \left(\frac{\sum \mathrm{Ar}_i}{\sum \mathrm{Ar}_m^+}\right) \longrightarrow \mathrm{Ar}_m^+ + \left(\frac{\sum \mathrm{Ar}_i}{\sum \mathrm{Ar}_m^+}\right) + e^-. \tag{59}$$

To confirm this last assertion, the results found for the ionization and recombination procedures for the complete CR model (optically thick case, $\theta = 2$, electronic and heavy particle collisions taken into account) are compared in Figure 5 with those obtained with a CR model considering only electronic collisions in the system of equation (55)). At high temperature ($T_e > 4200\,\mathrm{K}$), the results obtained by the two CR models are identical because

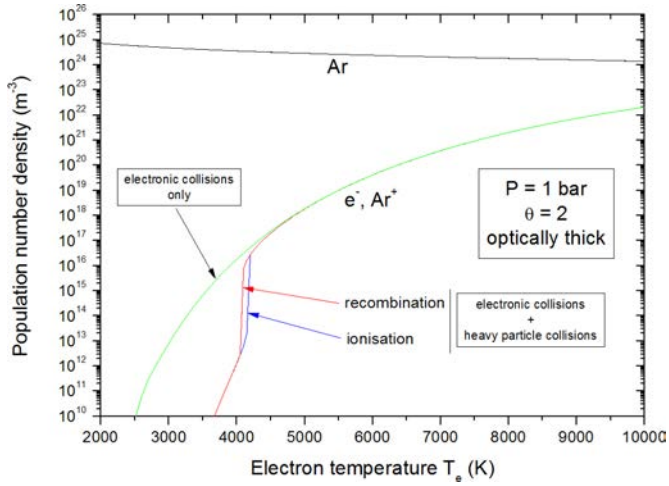

Fig. 5. Argon plasma composition: influence of electron and heavy particle collisions.

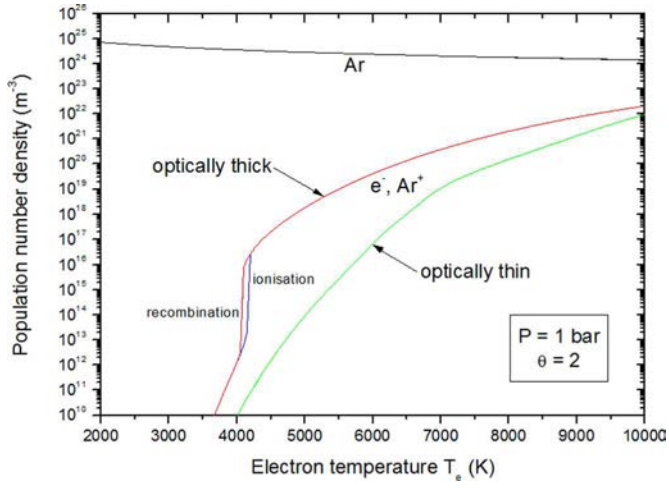

Fig. 6. Argon plasma composition: comparison between optically thick and thin cases.

electron collisions are dominant. On the other hand, at low temperature ($T_e < 4200\,\mathrm{K}$), the two series of results diverge because heavy particle reactions prevail when these processes are taken into account.

All the results presented in Figures 1–5 are obtained in an optically thick case ($\Lambda = 0$). To evaluate the influence of radiative processes, a comparison is made in Figure 6 between an optically thick argon plasma ($\Lambda = 0$, $\theta = 2$) and an optically thin case ($\Lambda = 1$, i.e. radiative processes introduced in the system of equation (55)). It should be noted that in the optically thin case, the ionization and recombination procedures lead to the same results whatever the temperature (no hysteresis formation). Thus only one result is presented in Figure 5 for the optically thin case.

In the optically thin case, electrons and Ar^+ ions are clearly underpopulated compared to the optically thick plasma. At the same time, neutral argon atoms are slightly overpopulated but this effect is not visible in Figure 6 because of the logarithmic scale chosen on the ordinate.

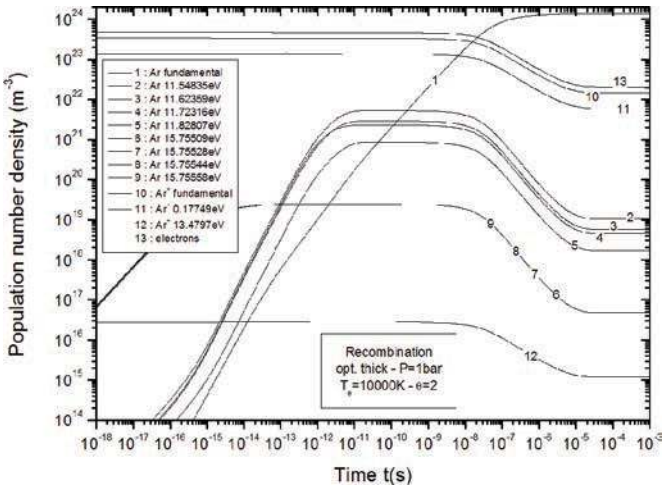

Fig. 7. Temporal evolution of some particular levels of Ar and Ar^+.

The underpopulation of electrons and ions in the optically thin case is associated with the radiative recombination process:

$$\mathrm{Ar}_m^+ + e^- \longrightarrow \mathrm{Ar}_i + h\nu. \tag{60}$$

This reaction is very efficient and it leads to a decrease of the population number density of charged particles in the plasma. However, it should be noted that the calculation performed in the optically thin case is realized with an escape factor $\Lambda = 1$ for all radiative processes. This means that all radiations escape from the plasma. This assumption is obviously not realistic. Indeed, the plasma is only partially optically thin but it is very difficult to fix an accurate value of the escape factor for each radiative process. As a consequence, the comparison in Figure 6 between the optically thick and optically thin cases gives the two extreme values of the possible compositions.

Finally, while this work is mainly devoted to the calculation of the steady state 2T plasma composition, it is also interesting to examine the temporal evolution of the population number densities of some particular levels or species during the convergence process.

The temporal profiles of the population number densities for the fundamental state of Ar, the first four excited levels (resonant levels) of Ar, the four highest excited levels of Ar, the fundamental state of Ar^+ and the two first excited levels of Ar^+ are presented in Figure 7. The characteristics of these levels (configurations and energies) are summarized in Table 1. The population number density of electrons is also given in Figure 7. The results presented in this figure correspond to a recombination case with an optically thick plasma with $P = 1\,\mathrm{bar}$, $T_e = 10\,000\,\mathrm{K}$ and $\theta = 2$.

The first observable result in Figure 7 is that population number densities corresponding to the steady state plasma composition are obtained for times higher than $10\,\mu\mathrm{s}$. Another interesting result is the formation of a quasi-steady-state (QSS) for all levels (except for the fundamental state of Ar) and electrons between 10^{-12} and

Table 1. Energies and configurations for some levels of Ar and Ar^+ [73].

Species	Configuration	Term	Quantum number J	Energy (eV)
Ar	$3s^2 3p^6$	1S	0	0.0
Ar	$3s^2 3p^5 ({}^2P^\circ_{3/2}) 4s$	$^2[3/2]$	2	11.54835433
Ar	$3s^2 3p^5 ({}^2P^\circ_{3/2}) 4s$	$^2[3/2]$	1	11.62359262
Ar	$3s^2 3p^5 ({}^2P^\circ_{1/2}) 4s$	$^2[1/2]$	0	11.72316029
Ar	$3s^2 3p^5 ({}^2P^\circ_{1/2}) 4s$	$^2[1/2]$	1	11.82807106
Ar	$3s^2 3p^5 ({}^2P^\circ_{3/2}) 55d$	$^2[3/2]$	1	15.75509
Ar	$3s^2 3p^5 ({}^2P^\circ_{3/2}) 56d$	$^2[3/2]$	1	15.75528
Ar	$3s^2 3p^5 ({}^2P^\circ_{3/2}) 57d$	$^2[3/2]$	1	15.75544
Ar	$3s^2 3p^5 ({}^2P^\circ_{3/2}) 58d$	$^2[3/2]$	1	15.75558
Ar^+	$3s^2 3p^5$	$^2P^\circ$	3/2	0.0
Ar^+	$3s^2 3p^5$	$^2P^\circ$	1/2	0.17749368
Ar^+	$3s 3p^6$	^2S	1/2	13.4797525

10^{-7} s. This kind of QSS behavior for population number densities of argon excited levels has already been observed by Bultel et al. [76]. As a consequence, in the present work, it is necessary to impose a relaxation time long enough to overtake the QSS composition in order to reach the real final steady-state (i.e. the steady-state 2T plasma composition).

4 Conclusion

A CR model has been developed to determine the composition of argon plasma in non-thermal equilibrium conditions. This CR model takes into account a large number of atomic levels of neutral argon (the 379 levels available in the NIST database [73]) and the first 7 states of Ar^+ ion up to 32.2 eV above the ground state of Ar. This selection of electronic levels for Ar and Ar^+ is coherent with the study of the plasma composition for temperatures T_e and T_h lower than 15 000 K.

The 2T plasma composition is obtained from the resolution of a non-linear system of equations constituted of 387 conservation equations (i.e. a balance equation for each considered electronic level and for electrons). This system of equations is dependent on the forward and backward reaction rate coefficients of inelastic collisions occurring in the plasma (excitation and ionization through electron and heavy particle impact in the present work). The system of equations also includes radiative mechanisms (spontaneous emission and radiative recombination) in the optically thin case.

Particular attention is paid in the present work to the formulation of accurate detailed balance relations allowing the computation of reverse reaction rate coefficients. Indeed, in the case of monoatomic plasmas (argon in the present case), the ionization phenomenon is controlled by two processes in competition with each other:

$$\mathrm{Ar} + e^- \longrightarrow \mathrm{Ar}^+ + 2e^- \tag{61}$$

$$\mathrm{Ar} + \mathrm{Ar} \longrightarrow \mathrm{Ar}^+ + \mathrm{Ar} + e^-. \tag{62}$$

There is no problem with the first mechanism as electrons are present on both sides. The second one is more problematic since there are only heavy particles in the forward direction, but electron and heavies in the reverse path. The balance relations calculated accurately in the present work (applying the micro-reversibility principle [79,80]) are different for the two processes. Indeed, these are two Saha-like equations but they do not depend on the same temperatures: only T_e for reaction (61) but T_e and T_h for process (62). This result confirms the non-uniqueness of the Saha-Eggert equation (ionization equilibrium) in the case of multi-temperature plasmas (and consequently the non-uniqueness of the law of mass action). As a consequence, in thermal nonequilibrium conditions, it is impossible to describe rigorously multi-T plasmas with a unique expression of a multi-T law of mass action. All these considerations concerning the detailed balance relations are taken into account in the CR model for the calculation of backward reaction rate coefficients.

The 2T compositions obtained in the optically thick case from the CR model exhibit abrupt modifications in the population number densities of electrons and Ar^+ ions. These sharp transitions are associated with the switch between the domination of the heavy particle reactions (at low temperature) and the predominance of the electron collisions (at high temperature). It is interesting to note that these abrupt transitions occur at different electron temperatures if the initial conditions of the CR model are set to values corresponding to ionization or recombination of the mixture. The consequence is the formation of a hysteresis-like area in the temperature range related to the sharp population number density changes. This result demonstrates the non-unicity of the solution for the 2T plasma composition in the temperature interval of the hysteresis-like zone. Indeed, population densities of electrons and ions are different in this temperature range in the case of ionization and recombination.

The introduction of the radiative processes in the CR model (optically thin case) has a significant effect on the population number densities of electrons and ions. These species are underpopulated when radiations are considered (mainly because of radiative recombination).

In the present work, the calculation of all direct reaction rate coefficients for excitation and ionization processes is performed with the well-known and widely used Drawin theory [75,77]. However, there are other available formulations in the literature allowing the determination

of atomic excitation and ionization rate coefficients. One can mention for example the works of Goldstein [84] for ionization, Giannaris and Incropera [85] and Van Regemorter [86] for excitation of optically allowed transitions, and Mansback and Keck [87] for forbidden transitions. In a forthcoming paper, these various theoretical approaches for reaction rate coefficient calculations will be used instead of the Drawin theory, in order to evaluate the influence of these different formulations on the 2T composition of monoatomic plasmas.

To continue the present work, it is also planned to use electronically and vibrationally specific CR models [64] to obtain accurate multi-temperature plasma compositions for molecular gases (such as O_2, N_2 and air). For this purpose, it will be necessary to study carefully some problematic chemical reactions involving molecules and molecular ions, with electrons and heavy particles on one side but only heavies on the other, such as:

$$\text{Dissociative recombination: } X_2^+ + e^- \leftrightarrow X + X \quad (63)$$

$$\text{Dissociative attachment: } X_2 + e^- \leftrightarrow X^- + X. \quad (64)$$

For these complex collisional processes, it will be necessary to attempt to establish detailed balance relations, or at least to define accurate calculation rules for the determination of backward rate coefficients.

Lastly, in future works, the 2T argon plasma compositions obtained in the present study will be used to calculate:

- first the associated thermodynamic properties (enthalpies and specific heat of electrons and heavy species);
- then the transport coefficients: viscosity, electrical conductivity and the various contributions (translation, internal and reaction) to thermal conductivities related to electrons and heavy particles;
- finally, the radiative properties such as the net emission coefficient [88–90] and mean absorption coefficients [91].

Author contribution statement

All authors were involved in the definition of this research project and participated to the discussion and the interpretation of the obtained numerical results. The calculations of the cross section and rate coefficient databases as well as the development of the CR model were mainly performed by J.A. All authors contributed significantly to the preparation and the improvement of the manuscript.

References

1. A. Gleizes, J.J. Gonzalez, P. Freton, J. Phys. D: Appl. Phys. **38**, R153 (2005)
2. J. Mostaghimi, P. Proulx, M.I. Boulos, J. Phys. D: Appl. Phys. **61**, 1753 (1987)
3. M. El Morsli, P. Proulx, J. Phys. D: Appl. Phys. **40**, 4810 (2007)
4. Y. Tanaka, J. Phys. D: Appl. Phys. **37**, 1190 (2004)
5. R. Ye, A.B. Murphy, T. Ishigaki, Plasma Chem. Plasma Process. **27**, 189 (2007)
6. S.A. Al-Mamun, Y. Tanaka, Y. Uesugi, Plasma Chem. Plasma Process. **30**, 141 (2010)
7. S. Ghorui, J.V.R. Heberlein, E. Pfender, J. Phys. D: Appl. Phys. **40**, 1966 (2007)
8. M. Boselli, V. Colombo, E. Ghedini, M. Gherardi, P. Sanibondi, J. Phys. D: Appl. Phys. **46**, 224009 (2013)
9. J.P. Trelles, J.V.R. Heberlein, E. Pfender, J. Phys. D: Appl. Phys. **40**, 5937 (2007)
10. Y. Bartosiewicz, P. Proulx, Y. Mercadier, J. Phys. D: Appl. Phys. **35**, 2139 (2002)
11. A. Kaminska, B. Lopez, B. Izrar, M. Dudek, Plasma Sources Sci. Technol. **17**, 035018 (2008)
12. M. Baeva, D. Uhrlandt, J. Phys. D: Appl. Phys. **46**, 325202 (2013)
13. P. Freton, J.J. Gonzalez, Z. Ranarijoana, J. Mougenot, J. Phys. D: Appl. Phys. **45**, 465206 (2012)
14. V. Colombo, E. Ghedini, M. Boselli, P. Sanibondi, A. Concetti, J. Phys. D: Appl. Phys. **44**, 194005 (2011)
15. J. Park, J.V.R. Heberlein, E. Pfender, G. Candler, C.H. Chang, Plasma Chem. Plasma Process. **28**, 213 (2008)
16. M.S. Benilov, G.V. Naidis, J. Phys. D: Appl. Phys. **36**, 1834 (2003)
17. V. Rat, Ph.D. thesis, University of Limoges, France, 2001 (in French)
18. V. Rat, P. André, J. Aubreton, M.F. Elchinger, P. Fauchais, D. Vacher, J. Phys. D: Appl. Phys. **35**, 981 (2002)
19. V. Rat, A.B. Murphy, J. Aubreton, M.F. Elchinger, P. Fauchais, J. Phys. D: Appl. Phys. **41**, 183001 (2008)
20. R.S. Devoto, Phys. Fluids **10**, 2105 (1967)
21. C. Bonnefoi, Ph.D. thesis no. 15-83, University of Limoges, France, 1983 (in French)
22. H.X. Wang, S.Q. Chen, X. Chen, J. Phys. D: Appl. Phys. **45**, 165202 (2012)
23. J. Aubreton, M.F. Elchinger, P. Fauchais, Plasma Chem. Plasma Process. **18**, 1 (1998)
24. W.Z. Wang, M.Z. Rong, J.D. Yan, A.B. Murphy, J.W. Spencer, Phys. Plasmas **18**, 113502 (2011)
25. S. Ghorui, J.V.R. Heberlein, E. Pfender, Plasma Chem. Plasma Process. **27**, 267 (2007)
26. W.Z. Wang, M.Z. Rong, Y. Wu, J.W. Spencer, J.D. Yan, D.H. Mei, Phys. Plasmas **19**, 083506 (2012)
27. S. Ghorui, J.V.R. Heberlein, E. Pfender, Plasma Chem. Plasma Process. **28**, 553 (2008)
28. V. Colombo, E. Ghedini, P. Sanibondi, Plasma Sources Sci. Technol. **20**, 035003 (2011)
29. V. Colombo, E. Ghedini E, P. Sanibondi, J. Phys. D: Appl. Phys. **42**, 055213 (2009)
30. J. Aubreton, M.F. Elchinger, V. Rat, P. Fauchais, J. Phys. D: Appl. Phys. **37**, 34 (2004)
31. V. Rat, P. André, J. Aubreton, M.F. Elchinger, P. Fauchais, A. Lefort, Plasma Chem. Plasma Process. **22**, 453 (2002)
32. V. Rat, P. André, J. Aubreton, M.F. Elchinger, P. Fauchais, A. Lefort, Plasma Chem. Plasma Process. **22**, 475 (2002)
33. J. Aubreton, M.F. Elchinger, J. Phys. D: Appl. Phys. **36**, 1798 (2003)
34. J. Aubreton, M.F. Elchinger, P. Fauchais, V. Rat, P. André, J. Phys. D: Appl. Phys. **37**, 2232 (2004)

35. W.B. White, S.M. Johnson, G.B. Dantzig, J. Chem. Phys. **28**, 751 (1958)
36. D. Godin, J.Y. Trépanier, Plasma Chem. Plasma Process. **24**, 447 (2004)
37. D.R. Bates, A.E. Kingston, R.W.P. McWhirter, Proc. R. Soc. Lond. Ser. A **267**, 297 (1962)
38. D.R. Bates, A.E. Kingston, R.W.P. McWhirter, Proc. R. Soc. Lond. Ser. A **270**, 155 (1962)
39. V. Rat, A.B. Murphy, J. Aubreton, M.F. Elchinger, P. Fauchais, J. Phys. D: Appl. Phys. **41**, 183001 (2008)
40. P. André, IEEE Trans. Plasma Sci. **23**, 453 (1995)
41. P. André, A. Lefort, J. Phys. D: Appl. Phys. **31**, 717 (1998)
42. X. Chen, P. Han, J. Phys. D: Appl. Phys. **32**, 1711 (1999)
43. P. André, J. Aubreton, M.F. Elchinger, V. Rat, P. Fauchais, A. Lefort, A.B. Murphy, Plasma Chem. Plasma Process. **24**, 435 (2004)
44. I. Prigogine, Bull. Cl. Sci. Acad. R. Belg. **26**, 53 (1940)
45. A.V. Potapov, High Temp. **4**, 48 (1966)
46. M.C.M. Van de Sanden, P.P.J.M. Schram, A.G. Peeters, J.A.M. Van der Mullen, G.M.W. Kroesen, Phys. Rev. E **40**, 5273 (1989)
47. Y. Tanaka, Y. Yokomizu, M. Ishikawa, T. Matsumura, IEEE Trans. Plasma Sci. **25**, 991 (1997)
48. A. Gleizes, B. Chervy, J.J. Gonzalez, J. Phys. D: Appl. Phys. **32**, 2060 (1999)
49. P. André, J. Aubreton, M.F. Elchinger, P. Fauchais, A. Lefort, Plasma Chem. Plasma Process. **21**, 83 (2001)
50. D. Giordano, M. Capitelli, Phys. Rev. E **65**, 016401 (2001)
51. J. Bacri, M. Lagreca, A. Médani, Physica B&C **113**, 403 (1982)
52. J.A. Kunc, W.H. Soon, Phys. Rev. A **40**, 5822 (1989)
53. L.C. Pierrot, C.O. Laux, C.H. Kruger, AIAA Paper AIAA 98-2664, in *Proceedings of the 29th Plasmadynamics and Lasers Conference, 1998, June 15–18, Albuquerque, NM, USA* (1998)
54. A.M. Gomes, A. Essoltani, J. Bacri, J. Quant. Spectrosc. Radiat. Transf. **43**, 471 (1990)
55. W.H. Soon, J.A. Kunc, Phys. Rev. A **41**, 825 (1990)
56. C.O. Laux, L. Yu, D.M. Packan, R.J. Gessman, L.C. Pierrot, C.H. Kruger, R.N. Zare, AIAA Paper AIAA 99-3476, in *Proceedings of the 30th Plasmadynamics and Lasers Conference, June 28–July 1, 1999, Norfolk, VA, USA* (1999)
57. Ph. Teulet, J.P. Sarrette, A.M. Gomes, J. Quant. Spectrosc. Radiat. Transf. **70**, 159 (2001)
58. M. Lino Da Silva, V. Guerra, J. Loureiro, Plasma Sources Sci. Technol. **18**, 034023 (2009)
59. A. Bultel, J. Annaloro, V. Morel, J. Phys.: Conf. Ser. **399**, 012014 (2012)
60. C. Park, *Nonequilibrium hypersonic aerothermodynamics* (Wiley, New York, 1990)
61. W.L. Hankey, *Re-entry aerodynamics. AIAA education series* (AIAA Inc., Washington, DC, 1988)
62. J.D. Anderson, *Hypersonic and high temperature gas dynamics* (McGraw-Hill, New York, 1989)
63. A. Bultel, B.G. Chéron, A. Bourdon, O. Motapon, I.F. Schneider, Phys. Plasmas **13**, 043502 (2006)
64. J. Annaloro, A. Bultel, Phys. Plasmas **21**, 123512 (2014)
65. A. Bultel, J. Annaloro, Plasma Sources Sci. Technol. **22**, 025008 (2013)
66. D.J. Drake, S. Popovic, L. Vuskovic, T. Dinh, IEEE Trans. Plasma Sci. **37**, 1646 (2009)
67. A.M. Brandis, C.O. Laux, T. Magin, T.J. McIntyre, R.G. Morgan, J. Thermophys. Heat Transf. **28**, 32 (2014)
68. P. André, Contrib. Plasma Phys. **37**, 23 (1997)
69. P. André, M. Abbaoui, R. Bessege, A. Lefort, Plasma Chem. Plasma Process. **17**, 207 (1997)
70. E. Richley, D.T. Tuma, J. Appl. Phys. **53**, 8537 (1982)
71. G.J. Cliteur, K. Suzuki, Y. Tanaka, T. Sakuta, T. Matsubara, Y. Yokomizu, T. Matsumura, J. Phys. D: Appl. Phys. **32**, 1851 (1999)
72. V. Rat, P. André, J. Aubreton, M.F. Elchinger, P. Fauchais, A. Lefort, J. Phys. D: Appl. Phys. **34**, 2191 (2001)
73. http://www.nist.gov/pml/data/asd.cfm
74. Y.B. Zel'dovich, Y.P. Raizer, *Physics of shock waves and high-temperature hydrodynamic phenomena* (Dover Mineola, New York, 2002)
75. H.W. Drawin, Collision and transport cross sections, Report EUR-CEA-FC 383, 1966
76. A. Bultel, B. Van Ootegem, A. Bourdon, P. Vervisch, Phys. Rev. E **65**, 046046 (2002)
77. H.W. Drawin, F. Emard, Phys. Lett. **43A**, 333 (1973)
78. C.O. Laux, Ph.D. thesis, Stanford University, HTGL Report T-288, 1993
79. A.R. Hochstim, *Kinetic processes in gases and plasmas* (Academic Press, New York, 1969)
80. J. Oxenius, *Kinetic theory of particles and photons* (Springer-Verlag, Berlin, 1986)
81. C.B. Collins, Phys. Rev. **158**, 94 (1967)
82. D.R. Bates, S.P. Khare, Proc. Phys. Soc. (Lond.) **85**, 231 (1965)
83. P.N. Brown, G.D. Byrne, A.C. Hindmarsh, SIAM J. Sci. Stat. Comput. **10**, 1038 (1989)
84. R. Goldstein, Numerical calculation of electron-atom excitation and ionization rates using Gryzinski cross sections, NASA Technical Report 32-1372, Jet Propulsion Laboratory, Pasadena, California, USA, 1969
85. R.J. Giannaris, F.P. Incropera, J. Quant. Spectrosc. Radiat. Transf. **11**, 291 (1971)
86. H.V.R. Van Regemorter, Astrophys. J. **136**, 906 (1962)
87. P. Mansbach, J. Keck, Phys. Rev. **181**, 275 (1969)
88. J.J. Lowke, E.R. Capriotti, J. Quant. Spectrosc. Radiat. Transf. **9**, 207 (1969)
89. J.J. Lowke, J. Quant. Spectrosc. Radiat. Transf. **14**, 111 (1974)
90. R.W. Libermann, J.J. Lowke, J. Quant. Spectrosc. Radiat. Transf. **16**, 253 (1976)
91. R. Hannachi, Y. Cressault, D. Salem, Ph. Teulet, L. Beji, Z. Ben Lakhdar, J. Phys. D: Appl. Phys. **45**, 485206 (2012)